

# Reservoir Memory Effect in the Establishment of Collective Emission: Non-Markovianity beyond Retardation

Yu-Xiang Zhang<sup>1,2,\*</sup>

<sup>1</sup>*Beijing National Laboratory for Condensed Matter Physics and Institute of Physics, Chinese Academy of Sciences, Beijing 100190, China*

<sup>2</sup>*School of Physical Sciences, University of Chinese Academy of Sciences, Beijing 100049, China*  
(Dated: April 4, 2023)

To establish a collective emission, the atoms in an ensemble must coordinate their behavior by exchanging virtual photons. We study this non-Markovian process in a subwavelength atom chain coupled to a one-dimensional (1D) waveguide and find that retardation is not the only cause of non-Markovianity. The other factor is the memory of the photonic environment, for which a single excited atom needs a finite time to cross from quadratic decay, the Zeno regime, to exponential decay. In waveguide setup, this crossover has a time scale longer than the retardation, thus impacts on the building up of collective behavior. By comparing a full quantum treatment with an approximation incorporating only the retardation effect, we find that field memory effect, characterized by the population of atomic excitation, is much more pronounced in collective emissions than that in the decay of a single atom.

It is well known since the 1960s [1, 2] that for an excited atom, the exponential decay derived from the Weisskopf-Wigner formalism [3] does not apply to the short-time dynamics: Due to the finite memory of the photonic reservoir, the decay rate is built up from zero quadratically at the first beginning [4, 5]. It has inspired the attempts to prohibit decaying by quickly repeating measurements [6–8], i.e., the Zeno effect. Actually, the duration of the non-exponential decay, characterized by the Zeno time  $\tau_Z$ , is typically many orders of magnitude shorter than the lifetime, rendering the field memory effect insignificant. For example, an optimal estimation of the 2P-1S transition of the hydrogen atom reads  $\tau_Z \sim 10^{-13}$ s [9]. Instead of the decay of a single atom, in this Letter, we shall show prominent reservoir memory effect in the formation of collective emissions from a subwavelength atom array, where the separation between two adjacent atoms,  $d$ , is shorter than the resonant wavelength  $\lambda$ .

Emission from an ensemble shows collective behavior because the atoms are interacting with a common radiation field [10]. For compact ensembles and weak atom-field couplings, collective behaviors are well described by Lehmburg's formalism based on the Markov approximation [11, 12]. For example, it predicts subradiant states with decay rates  $\gamma \propto N^{-\alpha}$  with  $N$  the number of atoms in subwavelength atom arrays [13–16]. However, Markovian theories are not able to describe the process of how the individual atoms are organized to eventually present a collective behavior. It is necessarily non-Markovian because of the retarded nature of photon-mediated atom-atom interaction. Then, a physical picture arises that the Markovian description is upgraded minimally by including the delayed feedback: Every atom starts from exponential decay independently and adjusts the decay rate in response to the signal from another atom. This picture has been studied for two atoms with the photonic reservoir being the free space [17] or 1D waveguide [18–

20]. Retardation effects of waveguide quantum electrodynamics (QED) are also studied in Refs. [21–26].

But how does the Zeno regime come into effect? We notice that the 2P-1S transition of the hydrogen atom has  $\tau_Z \gg 2\pi/\omega_0 \sim 10^{-15}$ s. In a subwavelength atom array, the minimal retardation time  $t_{\text{retard}} = d/c$ , with  $c$  the speed of light, satisfies the inequality that  $t_{\text{retard}} < \lambda/c = 2\pi/\omega_0 \ll \tau_Z$ . It means that the virtual photons sent from an atom have passed many other atoms, building up cooperativeness to a certain extent before the onset of exponential decay. Hence the establishment of collective emission and the reduction to Markovian behavior are simultaneous processes highly intertwined, as illustrated in Fig. 1(a). The scenario can be rephrased from the perspective of one atom in the array: The surrounding atoms play the role of observers that repeatedly alter its evolution every  $t_{\text{retard}}$ . Thus, the memory of the photonic reservoir must have nontrivial impacts on the establishment of collective emission.

To reveal it, we shall study the discrepancy between a full quantum treatment and the retardation-only picture mentioned above. This discrepancy is found to be much larger than the gap between the full quantum treatment of the decay of a single atom and the memory-less exponential decay, making subwavelength atom array a better system to detect the nontrivial properties of the photonic field. In this work we will focus on the system of waveguide QED. Possible experimental proposals and extensions to the memory effect of the free space radiation field will also be discussed.

*Zeno Time of the Waveguide QED.* The coupling between a 1D waveguide and two-level atoms with the ground state  $|g\rangle$  and excited state  $|e\rangle$  is conventionally described by a Hamiltonian in analogy with the multipolar gauge Hamiltonian of quantum optics, colloquially

the “ $\mathbf{d} \cdot \mathbf{E}$ ” Hamiltonian [27–29]

$$H_M = \sum_{i=1}^N \omega_0 \sigma_i^\dagger \sigma_i + \int_{-\Lambda}^{\Lambda} \frac{dk}{2\pi} \omega_k a_k^\dagger a_k - i \sum_{i=1}^N \int_{-\Lambda}^{\Lambda} \frac{dk}{2\pi} g_k \sigma_{i,X} (a_k e^{ikx_i} - a_k^\dagger e^{-ikx_i}) \quad (1)$$

where  $\sigma_i = |g\rangle_i \langle e|$ ,  $\sigma_{i,X} = \sigma_i + \sigma_i^\dagger$ ,  $\omega_k = v_g |k|$ ,  $v_g$  is the speed of light in the waveguide,  $g_k$  is the coupling strength to be specified,  $x_i$  denotes the coordinate of an atom, and  $v_g \Lambda$  is the spectrum cutoff (here the atomic transition is not near the photonic band edge [30]),  $a_k$  ( $a_k^\dagger$ ) is the bosonic annihilation (generation) operator satisfying the commutation relation  $[a_k, a_{k'}^\dagger] = 2\pi\delta(k - k')$  (all others vanish). We note that the bosons can also be surface acoustic waves [31, 32].

Since the rotating-wave approximation is not proper for short-time dynamics with a temporal resolution finer than  $t_{\text{prop}} < 2\pi/\omega_0$ , the counter-rotating terms of (1) cannot be ignored [9]. But the difficulties for theoretical treatment brought by them can be folded approximately by transforming the Hamiltonian to another gauge introduced by Drummond [33], which is also called the Jaynes-Cummings (JC) gauge [34, 35]. The unitary transformation from Hamiltonian (1) to the JC gauge is realized as  $H_{\text{JC}} = e^{-iS} H_M e^{iS}$  where

$$S = \sum_{i=1}^N \int_{-\Lambda}^{\Lambda} \frac{dk}{2\pi} \frac{g_k}{\omega_0 + \omega_k} \sigma_{i,X} (b_k e^{ikx_i} + b_k^\dagger e^{-ikx_i}). \quad (2)$$

At the first order of  $g_k$ , we obtain

$$H_{\text{JC}} = \sum_{i=1}^N \omega_0 \sigma_i^\dagger \sigma_i + \int_{-\Lambda}^{\Lambda} \frac{dk}{2\pi} \omega_k a_k^\dagger a_k - i \sum_{i=1}^N \int_{-\Lambda}^{\Lambda} \frac{dk}{2\pi} g_k^{\text{JC}} (\sigma_i^\dagger a_k e^{ikx_i} - \sigma_i a_k^\dagger e^{-ikx_i}) \quad (3)$$

where  $g_k^{\text{JC}} = 2g_k\omega_0/(\omega_k + \omega_0)$ . One can further introduce the corrections to  $\omega_0$  at the order of  $g_k^2$  to obtain a better approximation [36, 37].

An important property of  $H_{\text{JC}}$  is that the ground state of the full Hamiltonian  $|G\rangle = |g, \emptyset\rangle$  is identical to the ground state of the free Hamiltonian, where  $\emptyset$  denotes the field vacuum. In contrast, the same physical state reads  $e^{iS} |G\rangle$  for  $H_M$ , an entangled state between the atoms and the field. To coordinate the theoretical convention–dividing the Hilbert space into the atomic sector and the field sector and using an initial state in the product of them—with the laboratory practice of exciting atoms from the ground state of the full Hamiltonian (one can never turn off the atom-field interaction), we choose to work with  $H_{\text{JC}}$  in this work.

Next, we specify the coupling strength  $g_k$ . In the majority of literature, a local atom-field interaction is as-

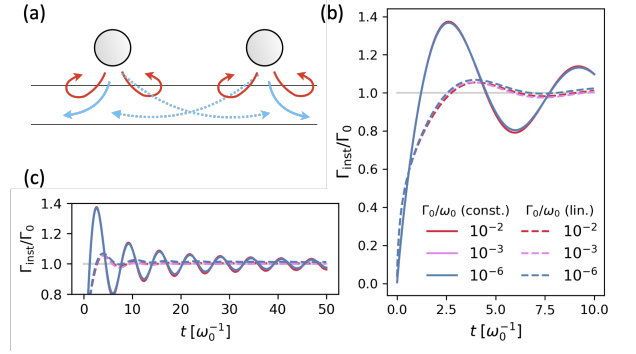


Figure 1. (a) Sketch of the idea: For closely separated atoms, the process of building up collective behaviors by exchanging virtual photons (dotted blue arrows) and the process to build up the Markovian decay rate  $\Gamma_0$  (due to the memory effect of the field represented by the red back-flow arrows) are highly intertwined. (b) The instantaneous emission rate of a single atom coupled to the waveguide,  $\Gamma_{\text{inst}}(t)$  (in the unit of  $\Gamma_0$ ) for  $t \leq 10/\omega_0$ . (c) Zoom-out view of (b) for  $t \leq 50/\omega_0$ .

sumed [38] so that  $g_k$  is a  $k$ -independent constant [27–29], which can be expressed through the Markovian decay rate  $\Gamma_0$  as  $g_k^2 = \Gamma_0 v_g/2$ . Another option is  $g_k \propto |k|^{1/2}$ , the same as the multipolar Hamiltonian of atoms in the free space [29] where the atoms couple to the transverse component of the displacement field [39]. Explicitly, we have  $g_k^2 = \Gamma_0 v_g |k|/(2k_0)$  with  $k_0 = \omega_0/v_g$ . Waveguide QED with the above two kinds of  $g_k$  has a constant and a linear spectral density, hence will be denoted by “const-wQED” and “lin-wQED”, respectively.

Now it is ready to calculate the Zeno time. Given an initial state  $|\Psi_0\rangle$  and a general unitary  $\exp(-iHt)$ , the Zeno time  $\tau_Z$  is defined from the short-time expansion of the non-decay probability

$$\left| \langle \Psi_0 | e^{-iHt} | \Psi_0 \rangle \right|^2 = 1 - t^2/\tau_Z^2 + \dots \quad (4)$$

The Zeno time is just a characterization but not exactly the duration of non-exponential decay. Nevertheless, we substitute  $H_{\text{JC}}$  and  $|e, \emptyset\rangle$  into Eq. (4) and obtain

$$\tau_Z^{-2} = \begin{cases} 2\Gamma_0\omega_0/\pi & \text{const.} \\ 2\Gamma_0\omega_0 \ln(\Lambda/k_0)/\pi & \text{lin.} \end{cases} \quad (5)$$

Remarkably,  $\tau_Z$  of const-wQED is  $\Lambda$ -independent. The above results imply that a subwavelength atom array has  $\tau_Z \gg 1/\omega_0$  provided the weak couplings  $\omega_0/\Gamma_0 \gg 1$  and  $\ln(\Lambda/k_0)$ , respectively.

*Equation of Motion.* Since  $H_{\text{JC}}$  preserves the number of excitations, we can use the singly-excited ansatz

$$|\Psi(t)\rangle = \sum_{i=1}^N \alpha_i(t) \sigma_i^\dagger |G\rangle + \int_{-\Lambda}^{\Lambda} \frac{dk}{2\pi} \beta_k(t) a_k^\dagger |G\rangle. \quad (6)$$

Then the Schrödinger equation in the interaction picture implies the following integro-differential equation for the

atomic amplitudes,

$$\frac{d}{dt}\alpha_i(t) = -\sum_{j=1}^N \int_{-\Lambda}^{\Lambda} \frac{dk}{2\pi} |g_k^{\text{JC}}|^2 \int_0^t d\tau \alpha_j(\tau) \times e^{ik(x_i-x_j)+i(\omega_k-\omega_0)(t-\tau)}. \quad (7)$$

See further manipulation of this equation in the Supplemental Material [40]. Both the amplitudes  $\alpha_i(t)$  and the photonic population  $\int |\beta_k|^2 dk/(2\pi)$  are calculated so that the normalization condition  $\langle \Psi(t) | \Psi(t) \rangle = 1$  can be used to reduce numerical error.

To have an idea of the field memory effect, we consider the decay of a single atom and plot in Figs. 1(b,c) the instantaneous decay rate  $\Gamma_{\text{inst}}(t) \equiv -\frac{d}{dt} \ln P_e(t)$ , where  $P_e(t)$  denotes the population in the atomic excited state. Therein, we apply three values of  $\Gamma_0/\omega_0$ , a slightly strong coupling  $10^{-2}$  and weak couplings  $10^{-3}$  and  $10^{-6}$ . The cutoff is set at  $\Lambda/k_0 = 10^4$ . We find that curves belonging to the three  $\Gamma_0/\omega_0$  almost overlap. For each value of  $\Gamma_0/\omega_0$ ,  $\Gamma_{\text{inst}}(t)$  of lin-wQED (dashed curve) increases faster at first ( $t \lesssim 1/\omega_0$ ) but soon becomes more gradual than  $\Gamma_{\text{inst}}(t)$  of const-wQED (solid curve). The later increases to roughly  $1.4\Gamma_0$  and starts to oscillate around  $\Gamma_0$  with a waning amplitude. As shown in Fig. 1(c), the oscillation is still visible at  $t = 50/\omega_0$ , equivalent to a propagation length of  $8\lambda$ .

In experiments, measuring  $\Gamma_{\text{inst}}(t)$  will be extremely demanding in the detector temporal resolution. If evidence of the memory effect can be obtained by measuring the change of population  $\Delta P_e(t) = P_e(t) - P_e(0)$  at some relatively large  $t$ , the requirement of temporal resolution can be significantly relaxed. However, due to the oscillations of  $\Gamma_{\text{inst}}(t)$ , it is perceivable, and will be shown in Fig. 2(e), that  $\Delta P_e(t)$  is quickly averaged out to the memory-less Markovian result.

Fortunately, we will see that it is not the case for collective emissions. To study the field memory effect while excluding the non-Markovianity attributed to retardation, Eq. (7) will be compared with the following one reproduced from Refs. [19, 20]

$$\frac{d}{dt}\alpha_i(t) = -\frac{\Gamma_0}{2} \left[ \alpha_i(t) + \sum_{j \neq i} e^{ik_0 r_{ij}} \alpha_j(t - \frac{r_{ij}}{v_g}) \Theta(t - \frac{r_{ij}}{v_g}) \right] \quad (8)$$

where  $r_{ij} = |x_i - x_j|$  and  $\Theta(t) = 1$  for  $t > 0$  and vanishes otherwise. One can derive this equation from Eq. (7) of either const-wQED or lin-wQED at the limit  $\Lambda \rightarrow \infty$  by an approximation presented in Ref. [17, 40]. Predictions of Eq. (8) is labeled by ‘‘retard.’’, remarking that it details the physical picture which goes beyond the Markovian formalism minimally by incorporating only the retardation effect.

*Superradiance.* We start from a chain of atoms initialized in the timed-Dicke state

$$|\Psi_k\rangle = \frac{1}{\sqrt{N}} \sum_{j=1}^N e^{ikx_j} \sigma_j^\dagger |G\rangle. \quad (9)$$

The preparation of such states is experimentally accessible [41, 42] and  $|\Psi_{k_0}\rangle$  is the single-photon superradiant state [43]. We assume  $N = 20$ ,  $\Gamma_0/\omega_0 = 10^{-4}$ , and a short atom-atom separation  $d = 0.1\pi/k_0$ . Larger values of  $d$  weaken the field memory effect. See results of  $d = 0.5\pi/k_0$  in the Supplemental Material [40]. The instantaneous decay rate of the whole chain predicted by Eqs. (7) and (8) are plotted in Fig. 2(a) for  $t \leq 10/\omega_0$ . The former shows continuous growth while the later gives a step-like increase. They agree well after  $t \approx 6/\omega_0$ .

Then we plot in Fig. 2(b) the instantaneous decay rate of five atoms in the chain, No. 1, 2, 5, 10, 20 ( $x_i < x_j$  if  $i < j$ ). It can be seen that they decay in different paces. Atom No. 1 decays slowly while Atom No. 20 accelerates to  $20\Gamma_0$ . The plots show agreement between the three

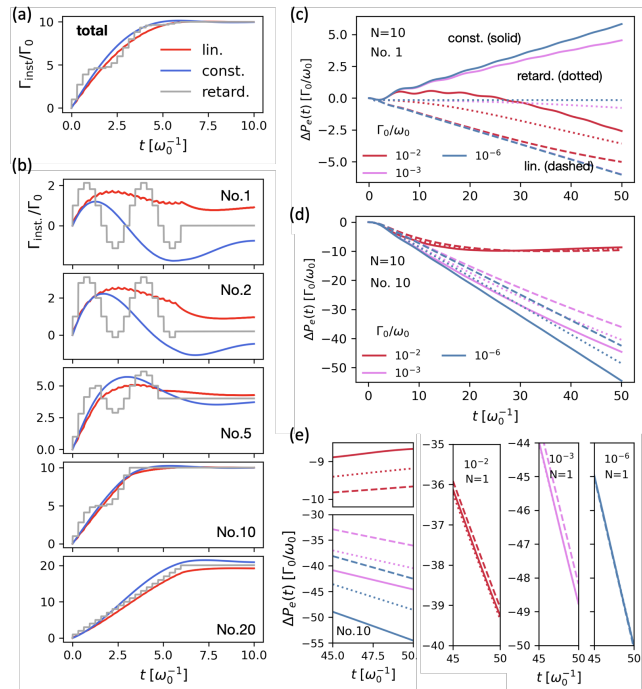


Figure 2. Decay of the superradiant timed-Dicke state  $|\Psi_{k_0}\rangle$ . (a) The instantaneous total decay rate  $\Gamma_{\text{inst}}(t)$  for  $\omega_0 t \in [0, 10]$  of a chain of 20 atoms with separation  $d = 0.1\pi/k_0$  and  $\Gamma_0/\omega_0 = 10^{-4}$ . (b) The instantaneous decay rate of five selected atoms [the legend is same as (a)]. (c)  $\Delta P_e(t)$  (in the unit of  $\Gamma_0/\omega_0$ ) of atom No. 1. The parameters are  $d = 0.1\pi/k_0$ ,  $N = 10$ , and  $\Gamma_0/\omega_0 = 10^{-2}$ ,  $10^{-3}$ , and  $10^{-6}$ . Predictions of Eq. (7) of the constant case, the linear case, and Eq. (8) are plotted by concrete, dashed, and dotted curves, respectively. (d) Same as (c) but for atom No. 10. (e) Left panel:  $\Delta P_e(t)$  of the last atom (No. 10) for  $\omega_0 t \in [45, 50]$ ; Right panels:  $\Delta P_e(t)$  of a single atom ( $N = 1$ ) coupled to the waveguide with  $\Gamma_0/\omega_0 = 10^{-2}$ ,  $10^{-3}$  and  $10^{-6}$ , respectively.

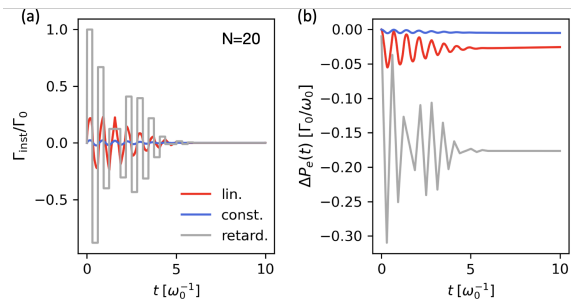


Figure 3. Decay of a subradiant eigenstate. (a) The instantaneous decay rate  $\Gamma_{\text{inst}}(t)$  (in the unit of  $\Gamma_0$ ) of 20 atoms initialized in  $|\Psi_{\text{sub}}\rangle$ . The other parameters are same as Fig. 2(a). (b) The total change of population on the excited state  $\Delta P_e(t)$  (in the unit of  $\Gamma_0/\omega_0$ ).

curves for atoms in the middle, i.e., atom No. 10, but not those near the ends. For Atom No. 1, the grey curve given by Eq. (8) shows two cycles of emission ( $\Gamma_{\text{inst}} > 0$ ) and absorption ( $\Gamma_{\text{inst}} < 0$ ) followed by an almost suppressed decay rate; the red curve of const-wQED shows only emission; the blue curve of lin-wQED exhibits emission at first but quickly turns to absorption.

To further illuminate the discrepancy, we plot  $\Delta P_e(t)$  of Atom No. 1 for a longer time window  $t \leq 50/\omega_0$  in Fig. 2(c). Note that an atom in state (9) has only  $1/N$  initial excitation. To avoid a too small  $\Delta P_e(t)$ , we assume a smaller chain of  $N = 10$  atoms. Meanwhile, to compare with the curves in Fig. 1, we consider the same three values of  $\Gamma_0/\omega_0$ . Figure 2(c) shows that for relatively weak couplings ( $\Gamma_0/\omega_0 = 10^{-3}$  and  $10^{-6}$ ) there is a gap of  $\lesssim 10\Gamma_0/\omega_0$  between the predictions of Eq. (7) of const-wQED and lin-wQED, while the predictions of Eq. (8) is roughly in the middle of them. Moreover, for const-wQED with  $\Gamma_0/\omega_0 = 10^{-2}$ , we can see the approaching to the prediction of Eq. (8) in the plotted regime. Similarly, we plot  $\Delta P_e(t)$  of the last atom (No. 10) in Fig. 2(d). It shows gaps of roughly the same scale (except for the case of  $\Gamma_0/\omega_0 = 10^{-2}$  where the atom-field coupling is stronger). A zoom-in view for  $\omega_0 t \in [45, 50]$  is given in the left-most panel of Fig. 2(e).

As promised above, we plot  $\Delta P_e(t)$  of the decay of a single atom for  $\omega_0 t \in [45, 50]$  in the right three panels of Fig. 2(e), in parallel to the curves of  $\Gamma_{\text{inst}}(t)$  in Fig. 1(b,c). We see that  $\Delta P_e(t)$  of const-wQED almost overlaps with the Markovian exponential decay, and  $\Delta P_e(t)$  of lin-wQED differs from them by much less than  $1\Gamma_0/\omega_0$ . Thus, in terms of  $\Delta P_e(t)$ , we conclude that the field memory effect is much more prominent in collective emissions than the decay of a single atom. Moreover, although our plots terminate at  $t = 50/\omega_0$ , a much larger  $t$  can be expected only after which the predictions of Eq. (7) tend toward the predictions of Eq. (8). Consequently, the temporal resolution needed to observe the field memory effect is significantly relaxed.

*Subradiance.* Now we study the decay of a subradiant state  $|\Psi_{\text{sub}}\rangle = (|\Psi_k\rangle - |\Psi_{-k}\rangle)/\sqrt{2}$  with  $kd = \pi N/(N+1)$ . It is an eigenstate of the effective non-Hermitian Hamiltonian obtained by the Markovian approximation [13–15]. We suppose the same parameters as in Fig. 2(a,b) and plot  $\Gamma_{\text{inst}}(t)$  of the whole chain in Fig. 3(a). In all cases, the subradiance is built through quick oscillations between emissions and absorptions. But the amplitudes of oscillation are different: the histogram-like curve of Eq. (8) has the largest amplitudes, while the amplitudes of const-wQED is the modest. In Fig. 3(b), we plot  $\Delta P_e(t)$  of the whole chain. It also shows apparent relative discrepancies between the three predictions. But because the state is subradiant, the values of  $\Delta P_e(t)$  are comparable to the decay of a single atom.

*Discussions.* It is of fundamental interest to extend from 1D waveguide to the 3D free space. But a controversial issue is on which Hamiltonian should all calculations be based. Most works chose the Coulomb gauge ( $\mathbf{A} \cdot \mathbf{p}$  interaction) disregarding the  $\mathbf{A}^2$  term, see, e.g., Refs. [44–48]. Other gauges are seldom used. And recently Hamiltonians of quantum optics, spontaneous emission rate and Lamb shift is revisited by causal perturbation theory [49]. Among them, the Coulomb-gauge Hamiltonian without both the  $\mathbf{A}^2$  term and the rotating-wave approximation gives  $\tau_Z^{-2} \sim \ln \Lambda$  [9], the same as lin-wQED. Thus, we expect the same field memory effect, or perhaps even more pronounced, because the resonant dipole-dipole interaction in the 3D free space diverges as  $1/r^3$  for short distances, giving rise to strong photon blockade [50]. In this sense, non-Markovianity beyond retardation of collective emissions from a small subwavelength atom array might be viewed as a probe to resolve which theory describes the real physics.

For experimental feasibility, the crux is to have a temporal resolution at the level of  $\omega_0^{-1}$  and subwavelength atom-atom separation. Among the various platforms of waveguide QED [29], the superconducting circuit works in the microwave regime with a centimeter-long wavelength. Thus, the requirement on a temporal resolution is not too harsh, and fabricating the transmon qubits into a subwavelength chain is straightforward [51].

*Conclusions.* We have studied the early stage of the decay of a collective excitation in subwavelength atom arrays coupled to a 1D waveguide. It is shown that retardation is not the only cause of non-Markovian effects, the memory of the photonic reservoir also strongly impact on the way how collective emissions are shaped. This is verified by calculations of the instantaneous decay rate and the change of population in the atomic excited state. In particular, the later (in the single-photon superradiant state) provides signals of memory effect more prominent than the decay of a single atom, and significantly relaxes the requirement on temporal resolution. For future works, one may inspect the non-Markovianity in collective emissions quantitatively using the tools of

non-Markovian open systems [52–54]. It is also important to study the possible experimental signatures of the memory effect of the 3D free space.

The author thanks Klaus Mølmer for valuable comments and acknowledges the financial support from the startup grant of IOP-CAS.

---

\* [iyxz@iphy.ac.cn](mailto:iyxz@iphy.ac.cn)

- [1] R. G. Winter, *Phys. Rev.* **123**, 1503 (1961).
- [2] R. G. Newton, *Annals of Physics* **14**, 333 (1961).
- [3] V. Weisskopf and E. Wigner, *Zeitschrift für Physik* **63**, 54 (1930).
- [4] S. R. Wilkinson, C. F. Bharucha, M. C. Fischer, K. W. Madison, P. R. Morrow, Q. Niu, B. Sundaram, and M. G. Raizen, *Nature* **387**, 575 (1997).
- [5] A. Crespi, F. V. Pepe, P. Facchi, F. Sciarrino, P. Mataloni, H. Nakazato, S. Pascazio, and R. Osellame, *Phys. Rev. Lett.* **122**, 130401 (2019).
- [6] C. B. Chiu, E. C. G. Sudarshan, and B. Misra, *Phys. Rev. D* **16**, 520 (1977).
- [7] B. Misra and E. C. G. Sudarshan, *Journal of Mathematical Physics* **18**, 756 (1977).
- [8] W. M. Itano, D. J. Heinzen, J. J. Bollinger, and D. J. Wineland, *Phys. Rev. A* **41**, 2295 (1990).
- [9] H. Zheng, S. Y. Zhu, and M. S. Zubairy, *Phys. Rev. Lett.* **101**, 200404 (2008).
- [10] R. H. Dicke, *Phys. Rev.* **93**, 99 (1954).
- [11] R. H. Lehmberg, *Phys. Rev. A* **2**, 883 (1970).
- [12] R. H. Lehmberg, *Phys. Rev. A* **2**, 889 (1970).
- [13] A. Asenjo-Garcia, M. Moreno-Cardoner, A. Albrecht, H. J. Kimble, and D. E. Chang, *Phys. Rev. X* **7**, 031024 (2017).
- [14] Y.-X. Zhang and K. Mølmer, *Phys. Rev. Lett.* **122**, 203605 (2019).
- [15] Y.-X. Zhang and K. Mølmer, *Phys. Rev. Lett.* **125**, 253601 (2020).
- [16] D. F. Kornovan, N. V. Corzo, J. Laurat, and A. S. Sheremet, *Phys. Rev. A* **100**, 063832 (2019).
- [17] P. W. Milonni and P. L. Knight, *Phys. Rev. A* **10**, 1096 (1974).
- [18] C. Gonzalez-Ballester, F. J. García-Vidal, and E. Moreno, *New Journal of Physics* **15**, 073015 (2013).
- [19] K. Sinha, P. Meystre, E. A. Goldschmidt, F. K. Fatemi, S. L. Rolston, and P. Solano, *Phys. Rev. Lett.* **124**, 043603 (2020).
- [20] K. Sinha, A. González-Tudela, Y. Lu, and P. Solano, *Phys. Rev. A* **102**, 043718 (2020).
- [21] F. Dinc and A. M. Brańczyk, *Phys. Rev. Res.* **1**, 032042 (2019).
- [22] H. Z. Shen, S. Xu, H. T. Cui, and X. X. Yi, *Phys. Rev. A* **99**, 032101 (2019).
- [23] A. Carmele, N. Nemet, V. Canela, and S. Parkins, *Phys. Rev. Res.* **2**, 013238 (2020).
- [24] S. Arranz Regidor, G. Crowder, H. Carmichael, and S. Hughes, *Phys. Rev. Res.* **3**, 023030 (2021).
- [25] R. Trivedi, D. Malz, S. Sun, S. Fan, and J. Vučković, *Phys. Rev. A* **104**, 013705 (2021).
- [26] K. Barkemeyer, A. Knorr, and A. Carmele, *Phys. Rev. A* **106**, 023708 (2022).
- [27] D. Roy, C. M. Wilson, and O. Firstenberg, *Rev. Mod. Phys.* **89**, 021001 (2017).
- [28] D. E. Chang, J. S. Douglas, A. González-Tudela, C.-L. Hung, and H. J. Kimble, *Rev. Mod. Phys.* **90**, 031002 (2018).
- [29] A. S. Sheremet, M. I. Petrov, I. V. Iorsh, A. V. Poshakinskiy, and A. N. Poddubny, “Waveguide quantum electrodynamics: collective radiance and photon-photon correlations,” (2021), [arXiv:2103.06824 \[quant-ph\]](https://arxiv.org/abs/2103.06824).
- [30] N. Vats and S. John, *Phys. Rev. A* **58**, 4168 (1998).
- [31] M. V. Gustafsson, T. Aref, A. F. Kockum, M. K. Ekström, G. Johansson, and P. Delsing, *Science* **346**, 207 (2014).
- [32] L. Guo, A. Grimsmo, A. F. Kockum, M. Pletyukhov, and G. Johansson, *Phys. Rev. A* **95**, 053821 (2017).
- [33] P. D. Drummond, *Phys. Rev. A* **35**, 4253 (1987).
- [34] A. Stokes and A. Nazir, *Nature Communications* **10** (2019), [10.1038/s41467-018-08101-0](https://doi.org/10.1038/s41467-018-08101-0).
- [35] A. Stokes and A. Nazir, *Rev. Mod. Phys.* **94**, 045003 (2022).
- [36] D.-w. Wang, Z.-h. Li, H. Zheng, and S.-y. Zhu, *Phys. Rev. A* **81**, 043819 (2010).
- [37] Y. Li, J. Evers, H. Zheng, and S.-Y. Zhu, *Phys. Rev. A* **85**, 053830 (2012).
- [38] J.-T. Shen and S. Fan, *Phys. Rev. Lett.* **95**, 213001 (2005).
- [39] C. Cohen-Tannoudji, J. Dupont-Roc, and G. Grynberg, *Photons and Atoms: Introduction to Quantum Electrodynamics*, 1st ed. (Wiley-VCH, 1997).
- [40] *Supplemental Material*.
- [41] R. Röhlsberger, K. Schlage, B. Sahoo, S. Couet, and R. Ruffer, *Science* **328**, 1248 (2010).
- [42] N. V. Corzo, J. Raskop, A. Chandra, A. S. Sheremet, B. Gouraud, and J. Laurat, *Nature* **566**, 359 (2019).
- [43] M. O. Scully, E. S. Fry, C. H. R. Ooi, and K. Wódkiewicz, *Phys. Rev. Lett.* **96**, 010501 (2006).
- [44] H. E. Moses, *Phys. Rev. A* **8**, 1710 (1973).
- [45] K. Wódkiewicz and J. Eberly, *Annals of Physics* **101**, 574 (1976).
- [46] J. Seke and W. N. Herfort, *Phys. Rev. A* **38**, 833 (1988).
- [47] P. Facchi and S. Pascazio, *Physics Letters A* **241**, 139 (1998).
- [48] P. R. Berman and G. W. Ford, *Phys. Rev. A* **82**, 023818 (2010).
- [49] K.-P. Marzlin and B. Fitzgerald, *Journal of Mathematical Physics* **59**, 042103 (2018).
- [50] A. Cidrim, T. S. do Espirito Santo, J. Schachenmayer, R. Kaiser, and R. Bachelard, *Phys. Rev. Lett.* **125**, 073601 (2020).
- [51] M. Mirhosseini, E. Kim, X. Zhang, A. Sipahigil, P. B. Dieterle, A. J. Keller, A. Asenjo-Garcia, D. E. Chang, and O. Painter, *Nature* **569**, 692 (2019).
- [52] Á. Rivas, S. F. Huelga, and M. B. Plenio, *Reports on Progress in Physics* **77**, 094001 (2014).
- [53] H.-P. Breuer, E.-M. Laine, J. Piilo, and B. Vacchini, *Rev. Mod. Phys.* **88**, 021002 (2016).
- [54] I. de Vega and D. Alonso, *Rev. Mod. Phys.* **89**, 015001 (2017).

## Supplemental Material

### A. Kernel of the Integro-Differential Equation

In our numerical calculations, the integro-differential equation (7) is transformed to an integral equation

$$\alpha_i(t) - \alpha_i(0) = i \frac{2\Gamma_0}{\pi} \int_0^t d\tau [A_{ij}(t - \tau)] \alpha_j(\tau), \quad (10)$$

$$A_{ij}^{\text{const.}}(\phi) = \int_0^\Lambda dx \frac{\cos(xr_{ij})}{(1+x)^2} \frac{1 - e^{i(1-x)\phi}}{x-1} = \frac{1}{4}(I_1 - I_2 - 2I_3), \quad (11)$$

and in the linear case,

$$A_{ij}^{\text{lin.}}(\phi) = \int_0^\Lambda dx \frac{x \cos(xr_{ij})}{(1+x)^2} \frac{1 - e^{i(1-x)\phi}}{x-1} = \frac{1}{4}(I_1 - I_2 + 2I_3); \quad (12)$$

where the abbreviated terms are

$$(I1) \int_0^\Lambda dx \frac{\cos(xr_{ij})}{x-1} (1 - e^{i(1-x)\phi}) = \left[ \cos(r_{ij}) \text{ci}(xr_{ij}) - \sin(r_{ij}) \text{si}(xr_{ij}) - \frac{e^{ir_{ij}}}{2} \text{csi}(xr_{ij}^-) - \frac{e^{-ir_{ij}}}{2} \text{csi}^*(xr_{ij}^+) \right] \Big|_{-1}^{\Lambda-1} \quad (13a)$$

$$(I2) \int_0^\Lambda dx \frac{\cos(xr_{ij})}{x+1} (1 - e^{i(1-x)\phi}) = \left[ \cos(r_{ij}) \text{ci}(xr_{ij}) + \sin(r_{ij}) \text{si}(xr_{ij}) - \frac{e^{i(\phi-r_{ij}^-)}}{2} \text{csi}(xr_{ij}^-) - \frac{e^{i(\phi+r_{ij}^+)}}{2} \text{csi}^*(xr_{ij}^+) \right] \Big|_1^{\Lambda+1} \quad (13b)$$

$$(I3) \int_0^\Lambda dx \frac{\cos(xr)}{(1+x)^2} [1 - e^{i(1-x)\phi}] = \frac{\cos(\Lambda r)}{\Lambda+1} (e^{-i(\Lambda+1)\phi} - 1) + 1 - e^{i\phi} - \left\{ r [\cos(r) \text{si}(xr) - \sin(r) \text{ci}(xr)] + \frac{i}{2} r_- e^{i(2\phi-r)} \text{csi}(xr_-) - \frac{i}{2} r_+ e^{i(2\phi+r)} \text{csi}^*(xr_+) \right\} \Big|_1^{\Lambda+1} \quad (13c)$$

where  $r_{ij}^\pm = r_{ij} \pm \phi$ , and we have introduced

$$\text{csi}(x) \equiv \text{ci}(x) + i \text{si}(x) \equiv - \int_x^\infty dt \frac{e^{it}}{t}.$$

The population of the bosonic field excitation

$$N_b(t) = \int_{-\Lambda}^\Lambda \frac{dk}{2\pi} |\beta_k(t)|^2$$

is obtained from the atomic amplitudes by

$$N_b(t) = \sum_{i,j=1}^N \int_0^t d\tau \int_0^t d\tau' B_{ij}(\tau - \tau') \alpha_i(\tau) \alpha_j(\tau'), \quad (14)$$

where the kernel is defined by

$$B_{ij}(t - \tau) = \int_{-\Lambda}^\Lambda \frac{dk}{2\pi} \left| g_k^{\text{JC}} \right|^2 e^{-ik(x_i - x_j) - i(\omega_0 - \omega_k)(t - \tau)} \quad (15)$$

where the kernel is specified in the below. To determine the kernels in the above integral equations, we introduce the unit less notations  $\phi = \omega_0(t - \tau)$ ,  $r_{ij} = k_0|x_i - x_j|$  and a short hand replacement  $\Lambda/k_0 \rightarrow \Lambda$ . Then we have that in the constant case,

For the constant case, the kernel of photon population is evaluated as

$$B_{ij}^{\text{const.}}(\phi) = \frac{\Gamma_0 \omega_0}{\pi} \int_0^\Lambda dx \frac{1}{(1+x)^2} 2 \cos(xr_{ij}) e^{i(x-1)\phi} = \frac{\Gamma_0 \omega_0 e^{-i\phi}}{\pi} \left[ - \frac{2 \cos(xr_{ij})}{1+x} e^{ix\phi} \Big|_0^\Lambda + \sum_{s=\pm} i\phi_s e^{-i\phi_s} \text{csi}(x\phi_s) \Big|_1^{\Lambda+1} \right] \quad (16)$$

where  $\phi_\pm = \phi \pm r_{ij}$ ; for the linear case, we have

$$B_{ij}^{\text{lin.}}(\phi) = \frac{\Gamma_0 \omega_0}{\pi} \int_0^\Lambda dx \frac{x}{(1+x)^2} 2 \cos(xr_{ij}) e^{i(x-1)\phi} = \sum_{s=\pm} e^{-i\phi_s} \text{csi}(x\phi_s) \Big|_1^{\Lambda+1} - B_{ij}^{\text{const.}}(\phi). \quad (17)$$

### B. Derivation of Eq. (8) of the main text

In the derivation of Eq. (8), the trick is to apply the approximation

$$\int \frac{dk}{2\pi} f(k) e^{i(k_0 - k)x} \approx f(k_0) \delta(x) \quad (18)$$

for a function  $f(k)$  that changes slowly with  $k$ . By this approximation, only the coupling strength at the resonant momentum,  $g_{k_0}$ , shows up in the end. Thus, there is no difference to start the derivation from either const-wQED or lin-wQED.

### C. Results of $d = 0.5\pi/d$

Results presented in the main text belong to sub-wavelength arrays with the atom-atom separation  $d = 0.1\pi/k_0$ . The field memory effect will be diminished if  $d$  becomes larger. To see it we consider a chain of 10 atoms with  $d = 0.5\pi/d$  and  $\Gamma_0/\omega_0 = 10^{-4}$ , and suppose the chain is initialized in the single-photon superradiant state  $|\Psi_{k_0}\rangle$ . We show in Fig. 4 the instantaneous decay

rate of the whole chain and of five atoms, No. 1, 2, 5, 6, 10. It can be seen that the differences between const-wQED, lin-wQED and Eq. (8) of the main text are less prominent than the case of  $d = 0.1\pi/k_0$ .

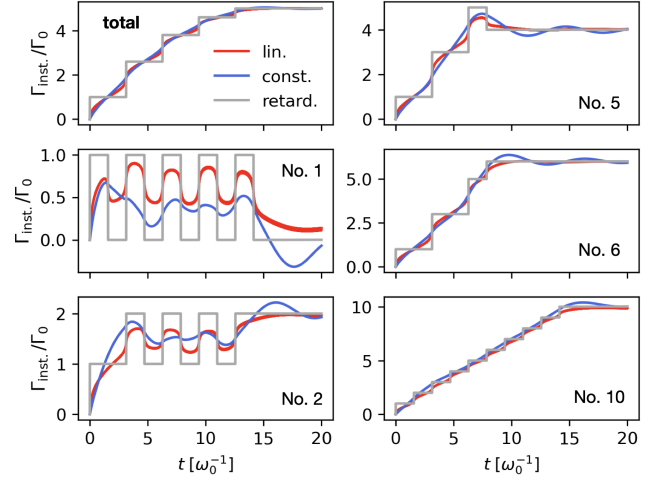


Figure 4. The instantaneous decay rate  $\Gamma_{\text{inst}}(t)$  (in the unit of  $\Gamma_0$ ) of a chain of 10 atoms initialized in  $|\Psi_{k_0}\rangle$  separated by  $d = 0.5\pi/k_0$ .